Simulating multidimensional optical wave-mixing signals with finite-pulse envelopes

Igor V. Schweigert and Shaul Mukamel
Department of Chemistry, University of California, Irvine, California 92697-2025, USA
(Received 13 September 2007; published 3 March 2008)

Closed expressions are derived for resonant coherent multidimensional spectra carried out with temporally well-separated pulses. The roles of the pulse carrier frequencies, phases, bandwidths, and envelopes can be readily analyzed. These results are particularly suitable for the design of new pulse sequences and for implementing coherent-control pulse-shaping algorithms for optimizing these signals to meet specific targets.

DOI: 10.1103/PhysRevA.77.033802 PACS number(s): 42.65.Re, 82.53.Kp, 78.47.−p

I. INTRODUCTION

Multidimensional optical $n+1$ wave-mixing spectroscopy [1–3] uses n laser pulses to generate a signal that is heterodyne detected with the last (local oscillator) pulse. The signals are usually plotted as 2D Fourier transforms with respect to two of the delay periods [4–10]. In addition to these delays, there are many other control parameters at one's disposal: the phase matching direction, pulse carrier frequencies, phases, and polarizations. Pulse-shaping techniques allow one to control all of the pulse envelopes [11–17]. Calculations of such signals are most easily performed in the impulsive limit where the pulses are taken to be much shorter than all other relevant time scales [18,19]. Impulsive signals only depend on the pulse delays and carrier frequencies. Pulse envelopes can then be incorporated by multiple convolutions of the impulsive signal with these envelopes [18].

In this paper we show that these multiple integrations can be eliminated under some general conditions and derive closed expressions for multidimsional optical signals that reveal their dependence on pulse envelopes. We consider a time-domain optical wave-mixing measurement carried out by subjecting the system to a sequence of temporally separated pulses

$$E(t)=\sum_{j=1}^{n+1}E_j(t). \tag{1}$$

The nonlinear polarization induced by interaction with the first n pulses is heterodyne detected by overlapping the signal field with the $n+1$ pulse. The signal is given by

$$S^{(n)}=\int_{-\infty}^{\infty}dtP^{(n)}(t)E_{n+1}(t). \tag{2}$$

If the pulses are suffiently weak, the order-by-order contributions to the nonlinear polarization are given by a perturbative expansion in the field

$$P^{(n)}(t)=\int_{-\infty}^{t}d\tau_n'\int_{-\infty}^{\tau_n'}d\tau_{n-1}'\cdots\int_{-\infty}^{\tau_2'}d\tau_1'R^{(n)}(t,\tau_n',\tau_{n-1}',\ldots,\tau_1')\times E(\tau_n')E(\tau_{n-1}')\cdots E(\tau_1'), \tag{3}$$

where the nonlinear response function $R^{(n)}$ is given by the combination of multitime correlation functions of the dipole operator [18]

$$R^{(n)}(t,\tau_n',\tau_{n-1}',\ldots,\tau_1')=\left(\frac{i}{\hbar}\right)^n\langle[\cdots[\hat{V}(t),\hat{V}(\tau_n')],\ldots,\hat{V}(\tau_1')]\rangle. \tag{4}$$

The response function is a pure material quantity which does not depend on the details of the optical measurement. It thus provides a convenient target for theoretical simulations. Calculating the nonlinear response according to Eq. (3) generally requires repeated evaluations the response function for various values of integration variables τ_j'. The calculations are considerably simplified in the impulsive limit by neglecting the finite duration of the pulses and setting $E_j(t)\sim E_j\delta(t-\tau_j)$. All time integrals are then eliminated and the signal is proportional to the response function itself

$$S^{(n)}=R^{(n)}(\tau_{n+1},\tau_n,\tau_{n-1},\ldots,\tau_1)E_{n+1}E_n\cdots E_1. \tag{5}$$

Equation (5) has been widely used for simulating time-domain measurements [1,2,16,20,21]. However, this equation is valid only if the pulses do not overlap

$$E_j(t)E_{j'}(t)=0 \quad \text{for each } j\neq j' \tag{6}$$

and if the system's time scales are much longer than the pulse durations (hence, the response function does not vary significantly during each pulse)

$$R^{(n)}(\ldots,\tau_j',\ldots)\approx R^{(n)}(\ldots,\tau_j,\ldots) \quad \text{for each } \tau_j' \text{ such that } E_j(\tau_j')\neq 0. \tag{7}$$

Only when both conditions (6) and (7) are satisfied can the finite duration of the pulse be safely neglected. While condition (6) is generally valid in sequential time-domain measurements, condition (7) may not necessarily be satisfied. In addition, if the response function is calculated by an expansion over eigenstates, Eq. (5) requires that all eigenstates be included as inifinely short pulses mathematically imply an infinite bandwidth. In order to implement the expression in a computationally tractable way one must truncate the summations over eigenstates based on physical considerations. For example, one can simply neglect all transitions lying outside the given bandwidths [22]. The signal then depends only on pulse delays and carrier frequencies.

In what follows, we show that the simple relation of Eq. (5) can be straightforwardly extended to describe sequential time-domain measurements even when the system's time scales are comparable with pulse durations. We show that for

 ©2008 The American Physical Society

nonoverlapping pulses, no additional assumption about the response function is necessary to formally carry out the integrations and derive closed expressions for the signals that include the finite pulse envelopes explicitly.

In Sec. II, we derive the expressions for the sequential time-domain measurements carried out with temporally seprated pulses with arbitrary envelopes when each pulse interacts with the system only once. This result is then extended in Sec. III to partially time ordered techniques such as pump probe where multiple interactions with each pulse are allowed.

II. TIME-ORDERED WAVE MIXING SIGNALS

We first focus on fully time-ordered techniques whereby each of the n pulses interacts only once with the system

$$S^{(n)} = \int_{-\infty}^{\infty} \tau'_{n+1} \int_{-\infty}^{\tau'_{n+1}} d\tau'_n \cdots \int_{-\infty}^{\tau'_2} d\tau'_1 \times R^{(n)}(\tau'_{n+1}, \ldots, \tau'_1) E_{n+1}(\tau'_{n+1}) E_n(\tau'_n) \cdots E_1(\tau'_1). \quad (8)$$

Since in such measurements, the product $E_{j+1}(t)E_j(t')$ vanishes unless $t > t'$, we can extend all upper integration limits in Eq. (8) to ∞, which gives

$$S^{(n)} = \left(\frac{i}{\hbar}\right)^n \langle [\cdots [\hat{V}_{n+1}, \hat{V}_n], \ldots, \hat{V}_1] \rangle, \quad (9)$$

where we have incorporated the time integrals into the definition of the interaction

$$\hat{V}_j \equiv \int d\tau E_j(\tau) \hat{V}(\tau). \quad (10)$$

The electric field of each pulse j can be generally represented in terms of its wave vector $\mathbf{k}_j$, carrier frequency ω_j, and the complex temporal envelope $\mathcal{E}_j$

$$E_j(t) = \mathcal{E}_j^+(t-\tau_j) e^{i\mathbf{k}_j \mathbf{r} - i\omega_j(t-\tau_j)} + \mathcal{E}_j^-(t-\tau_j) e^{-i\mathbf{k}_j \mathbf{r} + i\omega_j(t-\tau_j)}, \quad (11)$$

where $\mathcal{E}_j^+ = (\mathcal{E}_j^-)^* = \mathcal{E}_j$. Using Eq. (11), we define two operators

$$\hat{V}_j^{\pm}(\tau_j) \equiv \int d\tau \mathcal{E}_j^{\pm}(\tau) \hat{V}(\tau + \tau_j) e^{\mp i\omega_j \tau}. \quad (12)$$

This gives

$$\hat{V}_j \equiv V_j^+ + V_j^-. \quad (13)$$

In terms of these operators, we can recast the signal as

$$S^{(n)} = \sum_{\sigma=1}^{2^n} S_\sigma^{(n)}(\tau_{n+1}, \ldots, \tau_1), \quad (14)$$

where

$$S_\sigma^{(n)}(\tau_{n+1}, \ldots, \tau_1) = \left(\frac{i}{\hbar}\right)^n \langle [\cdots [\hat{V}_{n+1}^{\pm}(\tau_{n+1}), \hat{V}_n^{\pm}(\tau_n)], \ldots, \hat{V}_1^{\pm}(\tau_1)] \rangle, \quad (15)$$

and σ labels one of the possible 2^{n+1} combinations of $\{\hat{V}_{n+1}^{\pm}, \ldots, \hat{V}_1^{\pm}\}$.

Equations (14) and (15) extend Eq. (5) to include finite pulse envelopes. Since Eq. (12) depends the finite pulse duration, the corresponding expansion in eigenstates of $\hat{H}_0$ naturally accounts for the finite bandwidth

$$\hat{V}_j^{\pm}(\tau_j) \equiv \int d\tau \mathcal{E}_j^{\pm}(\tau) e^{\mp i\omega_j \tau} e^{i/\hbar \hat{H}_0(\tau+\tau_j)} \hat{V} e^{-i/\hbar \hat{H}_0(\tau+\tau_j)} = \sum_{\mu,\nu} \mathcal{E}_j^{\pm}(\omega_{\mu\nu} \mp \omega_j) e^{i\omega_{\mu\nu}\tau_j - \Gamma_{\mu\nu}\tau_j} \hat{V}_{\mu\nu}, \quad (16)$$

where $\hat{V}_{\mu\nu} = |\Psi_\mu\rangle V_{\mu\nu} \langle \Psi_\nu|$, $\omega_{\mu\nu}$, and $\Gamma_{\mu\nu}$ are, respectively, the frequency and dephasing rate of the transition between states Ψ_μ and Ψ_ν. $\mathcal{E}_j^{\pm}(\omega) \equiv \int d\tau \mathcal{E}_j^{\pm}(\tau) e^{i\omega\tau}$ is the frequency-domain envelope of the jth pulse. For example, for a Gaussian temporal envelope we have

$$\mathcal{E}_j^{\pm}(\tau) = \mathcal{E}_j^{\pm} e^{-\tau^2/T_j^2}, \quad \mathcal{E}_j^{\pm}(\omega) = \mathcal{E}_j^{\pm} \sqrt{\pi} T_j e^{-(\omega T_j)^2/4}. \quad (17)$$

Here, we assumed that pulse is shorter than the dephasing time and neglected the contribution of $\Gamma_{\mu\nu}$ to $\mathcal{E}_j^{\pm}(\omega)$.

Equation (16) provides the basis for the rotating-wave approximation, since the duration of an optical pulse T_j must be longer than its optical period (i.e., $T_j\omega_j > 2\pi$) and $\mathcal{E}_j(\omega + \omega_j) = 0$ for any positive ω. $\hat{V}_j^+$ thus describes an excitation since only terms with $\omega_{\mu\nu} > 0$ contribute, while V_j^- describes deexcitation as only terms with $\omega_{\mu\nu} < 0$ contribute to $\hat{V}_j^-$. Moreover, $\mathcal{E}_j(\omega)$ rapidly decays for $\omega \gg 1/T_j$ and thus only transitions in the vicinity of ω_j (within the bandwidth) contribute to resonant signals. Equation (16) is thus the finite-bandwidth extension of the rotating-wave approximation for a general sequential resonant optical measurement.

Equation (14) can be recast in a more compact form in terms of the delays between consecutive pulses $t_j \equiv \tau_{j+1} - \tau_j$

$$S^{(n)}(t_n, \ldots, t_1) = \sum_{\sigma=1}^{2^n} S_\sigma^{(n)}(t_n + \cdots + t_1, \ldots, t_2 + t_1, t_1, 0), \quad (18)$$

where we have used the invariance of $S_\sigma^{(n)}$ to time translation of all its arguments (see the Appendix).

Let us illustrate this result by the sum-over-states simulation of a four-wave mixing signal with the wave vector $\mathbf{k}_4 = \lambda_1\mathbf{k}_1 + \lambda_2\mathbf{k}_2 + \lambda_3\mathbf{k}_3$ and carrier frequency $\omega_4 = \lambda_1\omega_1 + \lambda_2\omega_2 + \lambda_3\omega_3$, where $\lambda_j = \pm 1$ represent the various possible phase-matching directions. The time-integrated signal [Eq. (18) with $n=3$] can be displayed as a multidimensional correlation plot in terms of the Fourier conjugates Ω_3, Ω_2, Ω_1 of the delay periods t_3, t_2, t_1

$$S_\sigma^{(3)}(\Omega_3,\Omega_2,\Omega_1) = \int\int\int_0^\infty dt_1 dt_2 dt_3 S_\sigma^{(3)}(t_3,t_2,t_1) e^{i\Omega_3 t_3 + i\Omega_2 t_2 + i\Omega_1 t_1}. \tag{19}$$

Using Eqs. (15)–(18) and the fact that $\omega_{\mu_4\nu_4} = -\omega_{\mu_3\nu_3} - \omega_{\mu_2\nu_2} - \omega_{\mu_1\nu_1}$ (see the Appendix) we get

$$\begin{aligned} S_\sigma^{(3)}(\Omega_3,\Omega_2,\Omega_1) = i \sum_{\mu_3\nu_3} \sum_{\mu_2\nu_2} \sum_{\mu_1\nu_1} & \frac{\mathcal{E}_4^-(\lambda_3\omega_3 + \lambda_2\omega_2 + \lambda_1\omega_1 - \omega_{\mu_3\nu_3} - \omega_{\mu_2\nu_2} - \omega_{\mu_1\nu_1}) \mathcal{E}_3^{\lambda_3}(\omega_{\mu_3\nu_3} - \lambda_3\omega_3)}{(\Omega_3 - \omega_{\mu_3\nu_3} - \omega_{\mu_2\nu_2} - \omega_{\mu_1\nu_1} + i\Gamma_{\mu_3\nu_3} + i\Gamma_{\mu_2\nu_2} + i\Gamma_{\mu_1\nu_1})} \\ & \times \frac{\mathcal{E}_2^{\lambda_2}(\omega_{\mu_2\nu_2} - \lambda_2\omega_2) \mathcal{E}_1^{\lambda_1}(\omega_{\mu_1\nu_1} - \lambda_1\omega_1)}{(\Omega_2 - \omega_{\mu_2\nu_2} - \omega_{\mu_1\nu_1} + i\Gamma_{\mu_2\nu_2} + i\Gamma_{\mu_1\nu_1})(\Omega_1 - \omega_{\mu_1\nu_1} + i\Gamma_{\mu_1\nu_1})} \\ & \times \langle [[[\hat{V}, \hat{V}_{\mu_3\nu_3}], \hat{V}_{\mu_2\nu_2}], \hat{V}_{\mu_1\nu_1}] \rangle, \end{aligned} \tag{20}$$

Equation (20) provides a convenient basis for designing and analyzing multidimensional spectra [23]. It explicitly reveals the dependence of the signal on the pulse parameters such as their shape ($\mathcal{E}_j$) and frequencies (ω_j). The four pulse envelopes guarantee that each pulse can only induce transitions lying within its bandwidth. Since all integrations have been eliminated the roles of all pulse control parameters can be readily discussed. Pulse shaping can be incorporated for applying coherent control algorithms for simplifying the spectra [24–26].

III. PARTIALLY TIME-ORDERED WAVE MIXING SIGNALS

We next extend these results to techniques involving multiple interactions with one of the pulses (labeled k):

$$\begin{aligned} S^{(n,m)} = & \int_{-\infty}^{\infty} d\tau'_{n+1} \int_{-\infty}^{\tau'_{n+1}} d\tau'_n \cdots \int_{-\infty}^{\tau'_{m+1}} d\tau_k^m \cdots \int_{-\infty}^{\tau_k^2} d\tau_k^1 \cdots \\ & \times \int_{-\infty}^{\tau'_2} d\tau'_1 R^{(n,m)}(\tau'_{n+1}, \tau'_n, \ldots, \tau'_1) \\ & \times E_{n+1}(\tau'_{n+1}) \cdots E_k(\tau_k^m) \cdots E_k(\tau_k^1) \cdots E_1(\tau'_1). \end{aligned} \tag{21}$$

Here, only the integration limits for $\tau'_1, \ldots, \tau'_n$ and τ_k^m can be set to ∞. Nevertheless, the signal can still be recast in the form of Eq. (14) with

$$S^{(n,m)} = \sum_{\sigma=1}^{2^n} S_\sigma^{(n,m)}(\tau_{n+1}, \ldots, \tau_1), \tag{22}$$

$$\begin{aligned} & S_\sigma^{(n,m)}(\tau_{n+1}, \ldots, \tau_1) \\ & = \left(\frac{i}{\hbar}\right)^{n+m-1} \int_{-\infty}^{\infty} d\tau'_m \cdots \int_{-\infty}^{\tau'_2} d\tau'_1 \mathcal{E}_k^{\pm}(\tau'_m) \cdots \mathcal{E}_k^{\pm}(\tau'_1) \\ & \quad \times \langle [\cdots [[\cdots [\hat{V}_{n+1}(\tau'_{n+1}), \hat{V}_n^{\pm}(\tau_n)], \ldots, \\ & \quad \hat{V}(\tau'_m + \tau_k)], \ldots, \hat{V}(\tau_1 + \tau_k)], \ldots, \hat{V}_1^{\pm}(\tau_1)] \rangle. \end{aligned} \tag{23}$$

Because the commutator in Eq. (23) includes some terms that do not correspond to the sequential ordering of operators $\hat{V}(\tau'_m + \tau_k) \cdots \hat{V}(\tau_1 + \tau_k)$, a compact definition similar Eq. (12) is not possible for these operators. Nevertheless, when the expansion over eigenstates is carried out, we get

$$\begin{aligned} S_\sigma^{(n,m)}(\tau_{n+1}, \tau_n, \ldots, \tau_1) = & \left(\frac{i}{\hbar}\right)^{n+m-1} \sum_{\mu_n,\nu_n} \cdots \sum_{\mu_1,\nu_1} \mathcal{E}_n^{\pm}(\omega_{\mu_n\nu_n} \mp \omega_n) \cdots \mathcal{E}_1^{\pm}(\omega_{\mu_1\nu_1} \mp \omega_1) \\ & \times \sum_{\mu'_m,\nu'_m}{}' \cdots \sum_{\mu'_1,\nu'_1}{}' \mathcal{E}_k^{\pm\cdots\pm}(\omega_{\mu'_k\nu'_k} \mp \omega_k, \ldots, \omega_{\mu'_1\nu'_1} \mp \omega_k) \\ & \times \langle [\cdots [[\cdots [\hat{V}, \hat{V}_{\mu_n\nu_n}], \ldots, \hat{V}_{\mu'_m\nu'_m}], \ldots, \hat{V}_{\mu'_1\nu'_1}], \ldots, \hat{V}_{\mu_1\nu_1}] \rangle. \end{aligned} \tag{24}$$

Here, the multipoint pulse envelope [27]

$$\mathcal{E}_k^{\pm\cdots\pm}(\Omega_m,\ldots,\Omega_1) = \int_{-\infty}^{\infty} d\tau'_m \int_{-\infty}^{\tau'_m} d\tau'_{m-1} \cdots \int_{-\infty}^{\tau'_2} d\tau'_1 \mathcal{E}_k^{\pm}(\tau'_m)\cdots\mathcal{E}_k^{\pm}(\tau'_1) \times e^{i\Omega_m\tau'_m+\cdots+i\Omega_1\tau'_1} \quad (25)$$

is expected to decay rapidly with increasing value of any of its arguments.

Let us illustrate this result for a sequential pump-probe measurement in a system whose states form a ladder of three manifolds (labeled g, e, and f in Fig. 1). The system interacts twice with the pump ω_1 and twice with the probe ω_2. The signal is defined as the difference in the probe absorption with and without the pump recorded as a function of the delay τ between pulses. Using Eq. (24), we find that only two terms contribute to the response function (Fig. 1)

$$S_{\mathrm{I}}^{(3)}(\tau) = \left(\frac{i}{\hbar}\right)^3 \sum_{\mu_4\nu_4}\cdots\sum_{\mu_1\nu_1} \mathcal{E}_2^{-+}(\omega_{\mu_4\nu_4}+\omega_2,\omega_{\mu_3\nu_3}-\omega_1) \times \mathcal{E}_1^{+-}(\omega_{\mu_2\nu_2}-\omega_1,\omega_{\mu_1\nu_1}+\omega_1) \times \langle[[[\hat{V}_{\mu_4\nu_4},\hat{V}_{\mu_3\nu_3}],\hat{V}_{\mu_2\nu_2}],\hat{V}_{\mu_1\nu_1}]\rangle \quad (26)$$

and

$$S_{\mathrm{II}}^{(3)}(\tau) = \left(\frac{i}{\hbar}\right)^3 \sum_{\mu_4\nu_4}\cdots\sum_{\mu_1\nu_1} \mathcal{E}_2^{-+}(\omega_{\mu_4\nu_4}+\omega_2,\omega_{\mu_3\nu_3}-\omega_1) \times \mathcal{E}_1^{-+}(\omega_{\mu_2\nu_2}+\omega_1,\omega_{\mu_1\nu_1}-\omega_1) \times \langle[[[\hat{V}_{\mu_4\nu_4},\hat{V}_{\mu_3\nu_3}],\hat{V}_{\mu_2\nu_2}],\hat{V}_{\mu_1\nu_1}]\rangle. \quad (27)$$

The signal is finally given by

$$\begin{aligned} S_{pp}(\omega_1,\omega_2,\tau) &= \mathrm{Im}[S_{\mathrm{I}}^{(3)}(\tau)+S_{\mathrm{II}}^{(3)}(\tau)] \\ &= \sum_{g,e,e'} \mathcal{E}_2^{-+}(\omega_{ge}+\omega_2,\omega_{e'g}-\omega_2)\mathcal{E}_1^{+-}(\omega_{eg_0}-\omega_1,\omega_{g_0e'}+\omega_1)V_{g_0e'}V_{e'g}V_{ge}V_{eg_0}e^{-i\omega_{ee'}\tau} \\ &+ \sum_{g,e,e'} \mathcal{E}_2^{-+}(\omega_{ge}+\omega_2,\omega_{eg_0}-\omega_2)\mathcal{E}_1^{+-}(\omega_{e'g}-\omega_1,\omega_{g_0e'}+\omega_1)V_{g_0e'}V_{e'g}V_{ge}V_{eg_0}e^{-i\omega_{g_0g}\tau} \\ &- \sum_{e,e',f} \mathcal{E}_2^{-+}(\omega_{e'f}+\omega_2,\omega_{fe}-\omega_2)\mathcal{E}_1^{+-}(\omega_{eg_0}-\omega_1,\omega_{g_0e'}+\omega_1)V_{g_0e'}V_{e'f}V_{fe}V_{eg_0}e^{-i\omega_{ee'}\tau} \\ &+ \sum_{g,e,e'} \mathcal{E}_2^{-+}(\omega_{ge}+\omega_2,\omega_{e'g}-\omega_2)\mathcal{E}_1^{-+}(\omega_{g_0e'}+\omega_1,\omega_{eg_0}-\omega_1)V_{g_0e'}V_{e'g}V_{ge}V_{eg_0}e^{-i\omega_{ee'}\tau} \\ &+ \sum_{g,e,e'} \mathcal{E}_2^{-+}(\omega_{g_0e'}+\omega_2,\omega_{e'g}-\omega_2)\mathcal{E}_1^{-+}(\omega_{ge}+\omega_1,\omega_{eg_0}-\omega_1)V_{g_0e'}V_{e'g}V_{ge}V_{eg_0}e^{-i\omega_{gg_0}\tau} \\ &- \sum_{e,e',f} \mathcal{E}_2^{-+}(\omega_{e'f}+\omega_2,\omega_{fe}-\omega_2)\mathcal{E}_1^{-+}(\omega_{g_0e'}+\omega_1,\omega_{eg_0}-\omega_1)V_{g_0e'}V_{e'f}V_{fe}V_{eg_0}e^{-i\omega_{ee'}\tau}, \end{aligned} \quad (28)$$

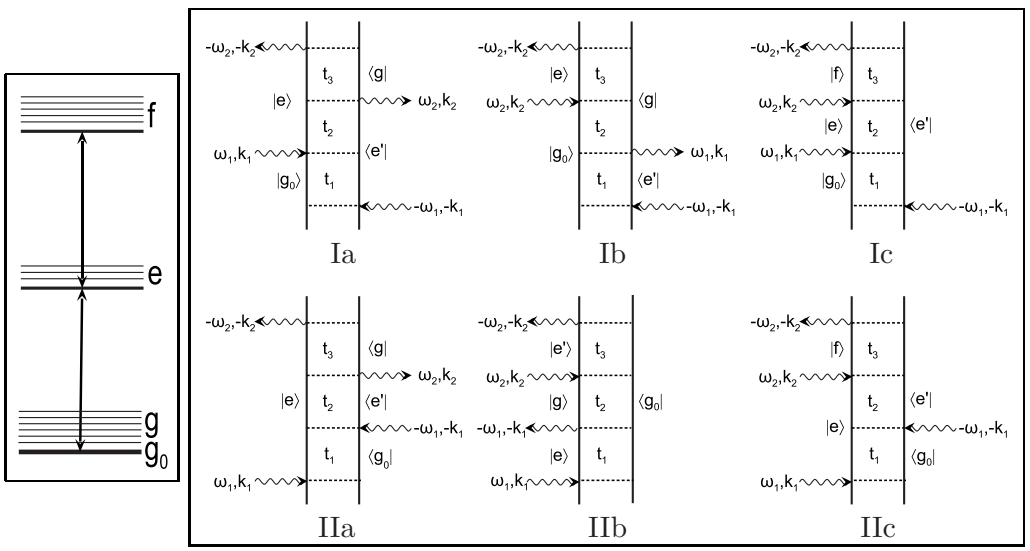

FIG. 1. Left panel, level scheme of the three excited-state manifolds. Right panel, double-sided Feynman diagrams representing the six terms contributing to the pump-probe signal [Eq. (29)].

where

$$\mathcal{E}_j^{\pm\pm}(\Omega_2,\Omega_1)=\int_{-\infty}^{\infty}d\tau_2'\int_{-\infty}^{\tau_2'}d\tau_1'\mathcal{E}_j^{\pm}(\tau_2')\mathcal{E}_j^{\pm}(\tau_1')e^{i\Omega_2\tau_2'+i\Omega_1\tau_1'}. \tag{29}$$

Similarly to Eq. (20), the two-point pulse envelope defined by Eq. (29) ensures that only the transitions within each pulse bandwidth contribute to the pump-probe signal in Eq. (28) (see, for example, Ref. [28]).

IV. CONCLUSIONS

We have derived closed expressions for multidimensional optical wave-mixing signals obtained with temporally well-separated pulses that accounts for finite pulse bandwidths. The sum-over-state expressions for resonant signals explicitly reveal the dependence on the carrier frequencies and spectral envolopes of the pulses. They thus provide a convenient basis for analyzing the role of various pulse parameters and can be used to design coherent control algorithms for optimizing these signals.

ACKNOWLEDGMENTS

We thank Dr. Darius Abramavicius for most useful discussions. The support of the Chemical Sciences, Geosciences, and Biosciences Division, Office of Basic Energy Sciences, Office of Science, U.S. Department of Energy is gratefully acknowledged.

APPENDIX

Each term contributing to the commutator in Eq. (4) is invariant to time translation of all its arguments

$$\begin{aligned}&\langle\hat{V}(\tau_{j_1}+\tau)\hat{V}(\tau_{j_2}+\tau)\cdots\hat{V}(\tau_{j_n}+\tau)\rangle\\&=\langle e^{i\hat{H}_0\tau}\hat{V}(\tau_{j_1})e^{-i\hat{H}_0\tau}e^{i\hat{H}_0\tau}\hat{V}(\tau_{j_2})e^{-i\hat{H}_0\tau}\cdots e^{i\hat{H}_0\tau}\hat{V}(\tau_{j_n})e^{-i\hat{H}_0\tau}\rangle\\&=\langle\hat{V}(\tau_{j_1})\hat{V}(\tau_{j_2})\cdots\hat{V}(\tau_{j_n})\rangle.\end{aligned} \tag{A1}$$

We thus have

$$R^{(n)}(\tau_{n+1}+\tau,\tau_n+\tau,\ldots,\tau_1+\tau)=R^{(n)}(\tau_{n+1},\tau_n,\ldots,\tau_1). \tag{A2}$$

Expanding $\hat{V}_j(\tau_j)$ in the eigenstates, we can recast Eq. (15) as

$$\begin{aligned}&S_\sigma^{(n)}(\tau_{n+1}+\tau,\ldots,\tau_1+\tau)\\&=\sum_{\mu,\nu}\sum_{\mu_n,\nu_n}\cdots\sum_{\mu_1,\nu_1}e^{i\omega_{\mu\nu}(\tau_{n+1}+\tau)}\cdots e^{i\omega_{\mu_1\nu_1}(\tau_1+\tau)}\\&\times\mathcal{E}_n^{\pm}(\omega_{\mu_n\nu_n}\mp\omega_n)\cdots\mathcal{E}_1^{\pm}(\omega_{\mu_1\nu_1}\mp\omega_1)\\&\times\langle[[\cdots[\hat{V}_{\mu\nu},\hat{V}_{\mu_n\nu_n}],\ldots,\hat{V}_{\mu_1\nu_1}]]\rangle,\end{aligned} \tag{A3}$$

where each of the terms contributing to the commutator has the following form:

$$\begin{aligned}&\langle\Psi_0|\Psi_{\mu_{j_{n+1}}}\rangle\langle\Psi_{\nu_{j_{n+1}}}|\Psi_{\mu_{j_n}}\rangle\cdots\langle\Psi_{\nu_{j_2}}|\Psi_{\mu_{j_1}}\rangle\langle\Psi_{\nu_{j_2}}|\Psi_0\rangle\\&=\delta_{\mu_{j_{n+1}},0}\delta_{\nu_{j_{n+1}},\mu_{j_n}}\cdots\delta_{\nu_{j_2},\mu_{j_1}}\delta_{\nu_{j_2},0},\end{aligned} \tag{A4}$$

where indices j_k label the operators in the order they appear in the given term. Since the sum over all $\omega_{\mu_{j_k}\nu_{j_k}}$ is independent on this order, we have

$$\begin{aligned}&\omega_{\mu_{n+1}\nu_{n+1}}+\omega_{\mu_n\nu_n}+\cdots+\omega_1\\&=\omega_{\mu_{j_{n+1}}\nu_{j_{n+1}}}+\omega_{\mu_{j_n}\nu_{j_n}}+\cdots+\omega_{\mu_{j_1}\nu_{j_1}}=\omega_{\mu_{j_{n+1}}\nu_{j_1}}=0.\end{aligned} \tag{A5}$$

This allows one to eliminate one of the $n+1$ pair of states contributing to Eq. (15). Relation (A5) is used to obtain Eq. (20).

[1] Y. Tanimura and S. Mukamel, J. Chem. Phys. **99**, 9496 (1993).
[2] S. Mukamel, Annu. Rev. Phys. Chem. **51**, 691 (2000).
[3] D. M. Jonas, Annu. Rev. Phys. Chem. **54**, 425 (2003).
[4] S. Mukamel and R. M. Hochstrasser, Chem. Phys. **266**, 135 (2001).
[5] M. C. Asplund *et al.*, Proc. Natl. Acad. Sci. U.S.A. **97**, 8219 (2000).
[6] P. Hamm and R. M. Hochstrasser, in *Ultrafast Infrared and Raman Spectroscopy*, edited by M. Fayer (Dekker, New York, 2001).
[7] P. F. Tian, D. Keusters, Y. Suzaki, and W. S. Warren, Science **300**, 1553 (2003).
[8] T. Brixner, J. Stenger, H. M. Vaswani, M. Cho, R. E. Blankenship, and G. R. Fleming, Nature (London) **434**, 625 (2005).
[9] J. R. Zheng, K. Kwak, J. Asbury, X. Chen, I. R. Piletic, and M. D. Fayer, Science **309**, 1338 (2005).
[10] X. Q. Li, T. H. Zhang, C. N. Borca, and S. T. Cundiff, Phys. Rev. Lett. **96**, 057406 (2006).
[11] A. M. Weiner, J. P. Heritage, and E. M. Kirschner, J. Opt. Soc. Am. B **5**, 1563 (1988).
[12] W. S. Warren, H. Rabitz, and M. Dahleh, Science **259**, 1581 (1993).
[13] D. Meshulach and Y. Silberberg, Nature (London) **396**, 239 (1998).
[14] A. Assion, T. Baumert, M. Bergt, T. Brixner, B. Kiefer, V. Seyfried, M. Strehle, and G. Gerber, Science **282**, 919 (1998).
[15] N. F. Scherer, L. D. Ziegler, and G. R. Fleming, J. Chem. Phys. **96**, 5544 (1992).
[16] M. H. Cho, N. F. Scherer, G. R. Fleming, and S. Mukamel, J. Chem. Phys. **96**, 5618 (1992).
[17] A. M. Weiner, Rev. Sci. Instrum. **71**, 1929 (2000).
[18] S. Mukamel, *Principles of Nonlinear Optical Spectroscopy* (Oxford University Press, New York, 1995).
[19] S. Mukamel and D. Abramavicius, Chem. Rev. **104**, 2073 (2004).
[20] Y. J. Yan and S. Mukamel, Phys. Rev. A **41**, 6485 (1990).

[21] L. Yang, I. V. Schweigert, S. T. Cundiff, and S. Mukamel, Phys. Rev. B **75**, 125302 (2007).
[22] A. M. Moran, S. M. Park, J. Dreyer, and S. Mukamel, J. Chem. Phys. **118**, 3651 (2003).
[23] I. V. Schweigert and S. Mukamel, Phys. Rev. Lett. **99**, 163001 (2007).
[24] D. Abramavicius and S. Mukamel, J. Chem. Phys. **120**, 8373 (2004).
[25] D. Voronine, D. Abramavicius, and S. Mukamel, J. Chem. Phys. **124**, 034104 (2006).
[26] D. Voronine, D. Abramavicius, and S. Mukamel, J. Chem. Phys. **125**, 224504 (2006).
[27] S. Mukamel, C. Ciordas-Ciurdariu, and V. Khidekel, Adv. Chem. Phys. **101**, 345 (1997).
[28] I. V. Schweigert and S. Mukamel, Phys. Rev. A **76**, 012504 (2007).